

# A multichannel superconducting soft x-ray spectrometer for high-resolution spectroscopy of dilute samples

S. Friedrich<sup>a)</sup>

Lawrence Berkeley National Laboratory, MS 6-2100, Berkeley, California 94720  
and Lawrence Livermore National Laboratory, L-418, Livermore, California 94551

T. Funk

Lawrence Berkeley National Laboratory, MS 6-2100, Berkeley, California 94720

O. Drury and S. E. Labov

Lawrence Livermore National Laboratory, L-418, Livermore, California 94551

S. P. Cramer

Lawrence Berkeley National Laboratory, MS 6-2100, Berkeley, California 94720  
and Department of Applied Science, EUIII, University of California, Davis, California 95616

(Presented on 23 August 2001)

We have built a high-resolution high-efficiency superconducting soft x-ray spectrometer for synchrotron-based fluorescence-detected absorption spectroscopy. The sensor is a  $3 \times 3$  array of  $200 \times 200 \mu\text{m}^2$  superconducting Nb–Al–Al<sub>2</sub>O<sub>3</sub>–Al–Nb tunnel junctions with an energy resolution around 15 eV below 1 keV and a total count rate capability of  $\approx 100\,000$  counts/s. This sensor array is cooled to  $\approx 0.1$  K by a two-stage adiabatic demagnetization refrigerator while held at the end of a 40-cm-long cold finger that can be inserted into an UHV sample chamber for x-ray fluorescence measurements. We present *L*-edge absorption spectra of dilute transition metals ( $\approx$  few 100 ppm) and discuss spectrometer performance with respect to the analysis of metalloproteins. © 2002 American Institute of Physics. [DOI: 10.1063/1.1445826]

## I. INTRODUCTION

X-ray absorption spectroscopy (XAS) samples atomic energy levels with sub-eV resolution by scanning the energy of a monochromatic synchrotron beam through an absorption edge of the element of interest. *L*-edge XAS is particularly insightful because natural line widths are smaller than at the *K* edges and because it utilizes dipole allowed transitions into the metal *3d* levels involved in the chemical binding. For concentrated samples, the absorption spectrum of the element of interest is typically obtained in x-ray transmission or electron yield measurements. For dilute samples, the sensitivity can be enhanced by measuring the intensity of the corresponding x-ray fluorescence (fluorescence-detected XAS), because the background can be greatly reduced if the fluorescence detector can discriminate the signal of interest from scatter and other fluorescence lines from the sample.<sup>1</sup>

Cryogenic x-ray detectors offer an advantage in the soft x-ray energy range when conventional semiconductor-based x-ray detectors cannot resolve the fluorescence line of interest from neighboring lines. Si(Li) or Ge detectors, for example, limit *L*-edge absorption spectroscopy on Mn and V sites in proteins because the weak *L* fluorescence is too close to the dominant O *K* and N *K* lines at 525 and 392 eV, respectively. Grating spectrometers, on the other hand, do offer the required energy resolution but lack the efficiency to collect data from dilute samples within an acceptable period

of time. This is crucial for biological samples that suffer from radiation damage.

We have built a cryogenic high-resolution x-ray detector system for synchrotron-based soft x-ray spectroscopy.<sup>2</sup> This development is motivated by interest in fluorescence-detected XAS of active metal sites in enzymes, as the fine structure in the absorption spectra can be related to the metal oxidation and spin state, its ligand environment, and thus to the enzymatic mechanism. Here we present the design of the cryostat, the performance of the superconducting detector array, and discuss the spectrometer capabilities for transition metal *L*-edge spectroscopy in metalloproteins.

## II. SPECTROMETER DESIGN

For the last five years, our groups at the Lawrence Berkeley and the Lawrence Livermore National Laboratories have collaborated to apply cryogenic high-resolution x-ray detectors in synchrotron-based research. We have focused on superconducting tunnel junction (STJ) detectors because their count rate capability of  $>10\,000$  counts/s per channel exceeds that of other cryogenic detector technologies by an order of magnitude.<sup>3,4</sup> Our STJ detectors consist of a 265 nm Nb base film, an Al–Al<sub>2</sub>O<sub>3</sub>–Al tunnel junction with 50 nm Al trapping layers and a 165 nm Nb absorber film. Their operating principle is similar to that of Si(Li) or Ge detectors, insofar as x rays excite excess charges above an energy gap in proportion to their energy, and the detector records an increase in current with a field-effect transistor-based pre-amplifier, followed by standard pulse shaping and data ac-

<sup>a)</sup>Corresponding author; electronic mail: sfriedrich@lbl.gov

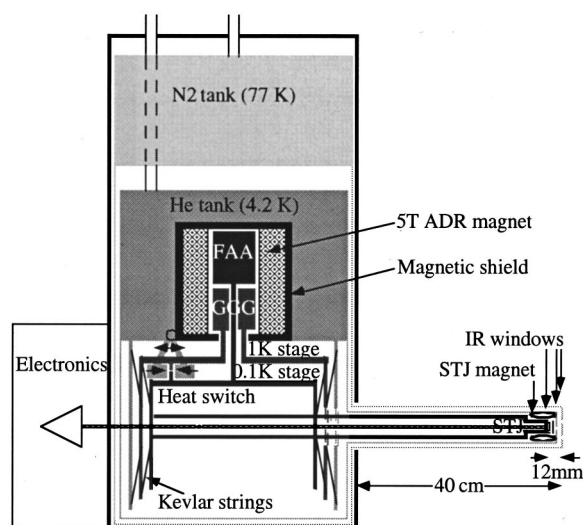


FIG. 1. Schematic of the two-stage ADR cryostat. The STJ detector array is held at the end of the detector cold finger  $\sim 12$  mm behind the end of the outer shield.

quisition electronics. One important difference is that the energy gap in superconductors is about a factor of 1000 smaller than in semiconductors, which translates into better charge statistics and thus better energy resolution. We have achieved an energy resolution as low as 1.7 eV full width at half maximum (FWHM) at 70 eV and 8.9 eV FWHM at 1 keV in our  $70 \times 70 \mu\text{m}^2$  STJs.<sup>5</sup> However, for the analysis of dilute samples it is advantageous to trade off some of this resolution for increased detector area. The spectrometer described here uses a  $3 \times 3$  array of  $200 \times 200 \mu\text{m}^2$  STJs with slightly lower resolution around  $\approx 15$  eV FWHM.

To operate the STJ array in synchrotron-based fluorescence applications, we have designed a two-stage adiabatic demagnetization refrigerator (ADR) that holds the array at the end of a 40-cm-long cold finger that can be inserted into an UHV vacuum chamber (Fig. 1).<sup>2,4,6</sup> It employs two nested cold stages, one cooled by gallium gadolinium garnet (GGG) to  $\approx 1$  K and a second one cooled by iron ammonium sulfate (FAA), to attain a base temperature of  $\approx 70$  mK without pumping on the liquid helium bath. For the operation of STJs no temperature stabilization is required, and the ADR hold time below the STJ's maximum operating temperature of  $\approx 0.4$  K is  $\approx 20$  h.

The cold finger is surrounded by two Au-plated oxygen-free high-conductivity Cu radiation shields, one liquid-He-cooled (which also supports a magnet to suppress the dc Josephson current) and one liquid-N<sub>2</sub>-cooled. Three thin windows in front of the STJ allow x-ray transmission while preventing infrared (IR) radiation from heating the cold stage and inducing shot noise. They consist of 200 Å Al on 1000 Å parylene, supported by a 90% transmissive Cu grid. The distance between the STJ detector array and the IR blocking window on the outermost radiation shield is  $\approx 12$  mm, so that the entire  $0.36 \text{ mm}^2$  array covers a solid angle  $\Omega/4\pi \approx 10^{-4}$  in typical experiments. The cryostat is compatible with UHV chamber pressure in the low  $10^{-9}$  mbar range during operation, and no residual gas freeze-out on the windows has been observed.

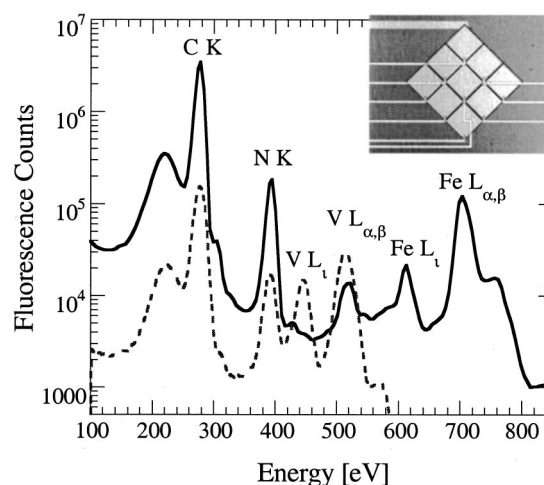


FIG. 2. Single pixel STJ fluorescence spectrum of vanadyl tetraphenyl porphyrin ( $\sim 2\%$  V, dashed) and of the same compound diluted with an iron-containing porphyrin to  $\sim 300$  ppm V (solid). The inset is a photograph of the  $3 \times 3$  STJ detector array.

### III. RESULTS AND DISCUSSION

The spectrometer is operated at beam line 4.0.2 of the Advanced Light Source at Lawrence Berkeley National Laboratory. We have examined a series of model compounds with varying V concentrations to determine the sensitivity of our spectrometer for vanadium  $L$ -edge spectroscopy. This is important for spectroscopy of V sites in proteins like V nitrogenase. Figure 2 shows fluorescence spectra from a single STJ of vanadyl tetraphenyl porphyrin ( $\approx 2\%$  V, dashed) and of the same compound diluted with an iron-containing porphyrin to  $\approx 300$  ppm V (solid). The energy resolution varies between 13 eV FWHM at C K and 17 eV at Fe  $L_t$ , and is comparable for the other pixels in the detector array. This is sufficient to separate the V  $L_\alpha$  and  $L_t$  fluorescence from other x-ray lines in the spectrum. The acquisition time for the dilute sample is about five times longer to improve the statistics of the weak V  $L$  signal.

For fluorescence-detected absorption spectroscopy, we define a region of multi-channel analyzer (MCA) channels around the V  $L$  fluorescence and count only the number of events in that region. The energy of the incident beam is stepped from 508 to 527 eV in 0.1 eV increments with an acquisition time of 10 s/point. The window for each MCA is chosen to optimize the signal-to-noise ratio for that pixel. We normalize the number of counts in that window by the incident flux  $I_0$  and subtract a linear background. The resulting absorption spectra (Fig. 3) have also been normalized to unity peak signal and offset for clarity. For the concentrated V sample, the spectrum has a signal-to-noise ratio, defined here as the maximum signal divided by the rms baseline noise below 512 eV, of about 500. This is more than sufficient to see the vanadium  $L_3$  and  $L_2$  edges corresponding to  $2p_{3/2} \rightarrow 3d$  and  $2p_{1/2} \rightarrow 3d$  transitions, respectively, as well as fine structure below the  $L_3$  edge. As expected, the signal-to-noise ratio is lower for another sample, an asphaltene with a vanadium concentration of  $\approx 2200$  ppm, despite the fact that three scans have been added for improved statistics. Still, the sensitivity is sufficient to analyze the spectral fine

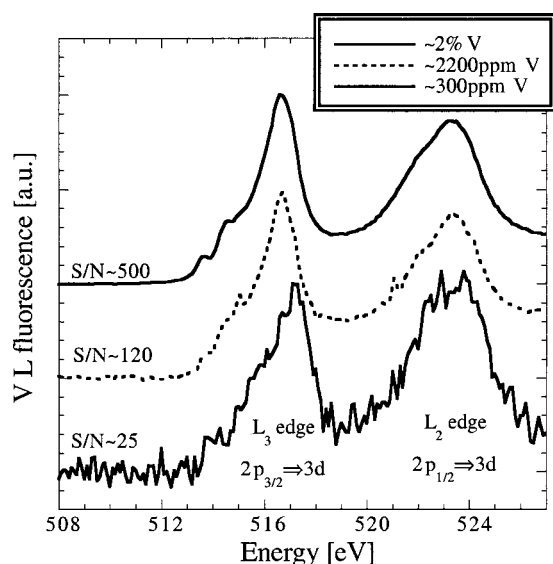


FIG. 3. Fluorescence-detected  $L$ -edge absorption spectrum of three V model compounds with different vanadium concentrations: vanadyl tetraphenyl porphyrin (solid, top), a V-containing asphaltene (dashed, middle), and V porphyrin diluted to 300 ppm V (solid, bottom).

structure. We note that absorption spectra on concentrated samples like these can also be taken by x-ray transmission or total electron yield.

Vanadium concentrations in metalloproteins are, unfortunately, much lower. To simulate a V site in a protein, we have examined the V porphyrin when diluted to a V concentration of 300 ppm by weight. At this concentration,  $L$ -edge transmission and total electron yield measurements are much more difficult, and fluorescence-detection is preferred. For the fluorescence-detected absorption spectrum in Fig. 3 we have added five scans (0.1 eV steps, 10 s/step) for improved statistics. The spectrum of the 300 ppm sample also shows the vanadium  $L_2$  and  $L_3$  edges, although the signal-to-noise ratio of 25 is not yet sufficient to observe fine structure in the  $L_3$  absorption edge. It is, however, sufficient to measure changes in absorption edge position of order 0.5 eV during

the catalytic cycle of a metalloprotein as the metal atom changes its oxidation state. The signal-to-noise ratio in this measurement is limited by the photon statistics of the background counts and can thus be further improved with longer acquisition time and larger or higher-efficiency detectors.

In summary, we have built a superconducting nine-channel soft x-ray spectrometer for synchrotron-based spectroscopy of dilute (few 100 ppm) systems. It offers an energy resolution of  $\approx 15$  eV FWHM, a maximum count rate above 100 000 counts/s, high quantum efficiency, and a solid angle coverage ( $\Omega/4\pi$ ) of  $\approx 10^{-4}$ . Our superconducting spectrometer is currently sufficiently sensitive to allow  $L$ -edge absorption spectroscopy on V (and also Mn and Ni) containing metalloenzymes at moderate concentrations. This allows high-resolution  $L$ -edge spectroscopy of active metal sites in metalloproteins and other dilute compounds. Future work will involve the development of larger detector arrays and the use of a polycapillary point-to-point focusing optic<sup>7</sup> for increased solid angle coverage.

#### ACKNOWLEDGMENTS

The authors gratefully thank J. D. Batteux for expert technical work, A. T. Young, E. Arenholz, S. Klingler, and the ALS support staff for valuable assistance with the beam line operation, and O. C. Mullins for providing the porphyrin and asphaltene samples. This work was performed under the auspices of the U.S. Department of Energy by University of California Lawrence Livermore National Laboratory under Contract No. W-7405-Eng-48. It was also supported by the DOE Office of Biological and Environmental Research and NIH GM44380.

<sup>1</sup>J. A. Jaclevic, M. P. Kirby, M. Klein, G. S. Brown, and P. Eisenberger, *Solid State Commun.* **23**, 679 (1977).

<sup>2</sup>S. Friedrich *et al.*, *Nucl. Instrum. Methods Phys. Res. A* **467-468**, 117 (2001).

<sup>3</sup>M. Frank *et al.*, *Rev. Sci. Instrum.* **69**, 25 (1998).

<sup>4</sup>D. A. Wollman, K. D. Irwin, G. C. Hilton, L. L. Dulcie, D. E. Newbury, and J. M. Martinis, *J. Microsc.* **188**, 196 (1997).

<sup>5</sup>S. Friedrich *et al.*, *IEEE Trans. Appl. Supercond.* **9**, 3330 (1999).

<sup>6</sup>C. Hagmann and P. L. Richards, *Cryogenics* **34**, 221 (1994).

<sup>7</sup>N. Gao *et al.*, *Appl. Phys. Lett.* **71**, 3441 (1997).